

# Mechanistical studies on the formation of isotopomers of hydrogen peroxide (HOOH), hydrotrioxy (HOOO), and dihydrogentrioxide (HOOOH) in electron-irradiated H<sub>2</sub><sup>18</sup>O/O<sub>2</sub> ice mixtures†

Weijun Zheng,<sup>ab</sup> David Jewitt<sup>a</sup> and Ralf I. Kaiser<sup>\*b</sup>

Received 18th January 2007, Accepted 26th February 2007

First published as an Advance Article on the web 13th March 2007

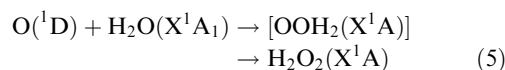
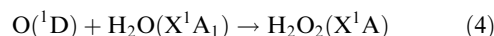
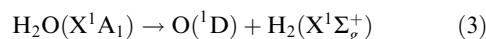
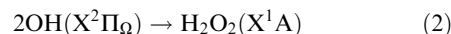
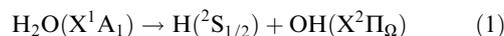
DOI: 10.1039/b700814g

In order to investigate the chemical reactions inside water–oxygen ice mixtures in extreme environments, and to confirm the proposed reaction mechanisms in pure water ice, we conducted a detailed infrared spectroscopy and mass spectrometry study on the electron irradiation of H<sub>2</sub><sup>18</sup>O/O<sub>2</sub> ice mixtures. The formation of molecular hydrogen, isotopically substituted oxygen molecules <sup>18</sup>O<sup>18</sup>O and <sup>16</sup>O<sup>18</sup>O, ozone (<sup>16</sup>O<sup>16</sup>O<sup>16</sup>O, <sup>16</sup>O<sup>16</sup>O<sup>18</sup>O, and <sup>16</sup>O<sup>18</sup>O<sup>16</sup>O), hydrogen peroxide (H<sup>18</sup>O<sup>18</sup>OH, H<sup>16</sup>O<sup>16</sup>OH and H<sup>16</sup>O<sup>18</sup>OH), hydrotrioxy (HOOO), and dihydrogentrioxide (HOOOH) were detected. Kinetic models and reaction mechanisms are proposed to form these molecules in water and oxygen-rich solar system ices.

## 1. Introduction

During the last decade, experimental studies on the charged-particle irradiation of amorphous and crystalline water ices (H<sub>2</sub>O) have received considerable attention.<sup>1–10</sup> This research is triggered by the interest of physical chemists and solar system scientists to understand how energetic particles like electrons, protons, helium, carbon, nitrogen, oxygen, and sulfur ions with kinetic energies up to a few ten keV, as present in the solar wind and planetary magnetospheres, induce non-equilibrium chemistry upon interacting with water-rich surfaces of icy moons like Europa, Ganymede, and Callisto<sup>11</sup> as well as of Kuiper Belt Objects (KBOs) like Quaoar.<sup>12,13</sup> These simulation experiments also hold strong links to the cosmic ray processing of interstellar ices as present on water-rich grain particles in cold molecular clouds.<sup>4,14</sup> Upon the implantation of, for instance, MeV protons into molecular solids like water, methane, and ammonia, the primary energy loss of the implant is *via* inelastic energy transfer processes. This can lead to vibrational excitation, bond ruptures, and ionization of the target molecules ultimately generating a cascade of secondary electrons in the icy grain mantle.<sup>15,16</sup> Qualitatively spoken, there is a general consensus that the charged particle and photon processing of neat water ices produces atomic and molecular hydrogen (H, H<sub>2</sub>), atomic and molecular oxygen (O, O<sub>2</sub>), the hydroxyl radical (OH), and hydrogen peroxide (H<sub>2</sub>O<sub>2</sub>).<sup>1,4,7,17</sup> The actual production rates, however, depend strongly on the temperatures (10 K–140 K), the ice structure and morphology (crystalline *versus* amorphous), the irradiating particle (the linear energy transfer of the implant to the water ice), and the dose. A comprehensive compilation of irradiation experiments of pure water ices has been given

recently by Zheng *et al.*<sup>18</sup> Various reaction mechanisms (eqn (1)–(5)) have been proposed to kinetically fit the temporal evolution of the column densities of hydrogen peroxide formed in water ices.<sup>18,19</sup> Two mechanisms currently in favor are the recombination of two hydroxyl radicals formed *via* unimolecular decomposition of the water molecule (eqn (1)–(2)) and the reaction of electronically excited oxygen atoms, O(<sup>1</sup>D), with water either *via* an insertion (reaction (4)) or through an oxywater intermediate OOH<sub>2</sub>(X<sup>1</sup>A) (reaction (5)). The branching ratios of the processes (1)/(2) *versus* (3)/(4)/(5) are currently unknown.



In this paper, we focus on the mechanistic aspect of the formation of hydrogen peroxide in water ices, and attempt to elucidate to what extent hydrogen peroxide is formed *via* recombination of two hydroxyl radicals or *via* reaction of an electronically excited oxygen atom with a second water molecule. To actually ‘trace’ the oxygen atom, we conducted experiments on H<sub>2</sub>/<sup>18</sup>O–<sup>16</sup>O<sub>2</sub> mixtures. Here, oxygen atoms can be liberated from the water molecule forming <sup>18</sup>O or from molecular oxygen giving <sup>16</sup>O.<sup>20</sup>

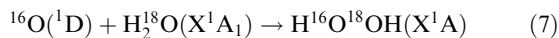
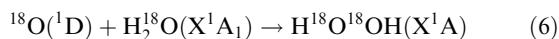
Therefore, if these oxygen atoms react with a neighboring H<sub>2</sub><sup>18</sup>O molecule solely *via* eqn (4) and/or (5), the formation of hydrogen peroxide should proceed *via* eqn (6) and (7). Therefore, a detection of H<sup>18</sup>O<sup>18</sup>OH(X<sup>1</sup>A) and H<sup>16</sup>O<sup>18</sup>OH(X<sup>1</sup>A) would indicate that oxygen atoms can react with water to

<sup>a</sup> Institute for Astronomy, University of Hawaii at Manoa, Honolulu, HI 96822

<sup>b</sup> Department of Chemistry, University of Hawaii at Manoa, Honolulu, HI 96822. E-mail: kaiser@gold.chem.hawaii.edu

† The HTML version of this article has been enhanced with colour images.

form hydrogen peroxide. On the other hand, a synthesis of hydrogen peroxide *via* recombination of two hydroxyl radicals would yield solely  $\text{H}^{18}\text{O}^{18}\text{OH}(\text{X}^1\text{A})$  (eqn (8)).



Recall that these formation routes to hydrogen peroxide involve pseudo-first order kinetics.<sup>18,19</sup> However, in case of water–oxygen mixtures, various multi-step formation routes to hydrogen peroxide that may complicate the situation have to be considered as well. First,  $^{16}\text{O}$  and  $^{18}\text{O}$  may abstract a hydrogen atom from water to form a  $^{16}\text{OH}$  and  $^{18}\text{OH}$  radical,<sup>21,22</sup> respectively, leading *via* recombination of a second hydroxyl radical to hydrogen peroxide. However, these processes are expected to follow higher-order kinetics. Likewise, the stepwise addition of two hydrogen atoms to molecular oxygen *via* a HOO intermediate can also form hydrogen peroxide. Similarly to the abstraction sequence, this reaction would also require higher order kinetics *via* a consecutive reaction sequence. Finally, reactions of  $^{18}\text{O}$  with molecular oxygen could also lead to an isotopic exchange forming  $^{16}\text{O}^{18}\text{O}$ , which in turn would give  $\text{H}^{16}\text{O}^{18}\text{OH}$  *via* two hydrogen atom additions. Nevertheless, this process would be an even higher order reaction sequence than the stepwise addition of two hydrogen atoms to molecular oxygen. Therefore, by identifying isotopomers of hydrogen peroxide and following their kinetics, we should be able to provide much needed insight on the reaction mechanism(s) to form hydrogen peroxide in charged particle-processed water-rich ices.

Note that solid, molecular oxygen is also an important component of interstellar ice and solar system ice.<sup>23</sup> In our solar system, molecular oxygen has been identified explicitly on the surfaces of the Jovian satellites Europa and Ganymede based on the absorption bands at 577 nm and 627.5 nm.<sup>24,25</sup> Both water and oxygen are also important for the origin of life and the astrobiological evolution of the interstellar medium.<sup>26,27</sup> Only a few previous studies exist on the irradiation of water–oxygen mixtures. Cooper *et al.*<sup>28</sup> reported the formation of  $\text{HO}_2$  and  $\text{HO}_3$  radicals in water/oxygen ice mixture irradiated with 0.8 MeV protons. Moore and Hudson<sup>1</sup> also observed the formation of ozone in water–oxygen mixtures. However, no ozone was formed in pure water ice. Therefore, our present experiments not only provide reaction mechanisms to form hydrogen peroxide, but also investigate alternative chemical reactions inside water–oxygen ice mixtures in extreme environments.

## 2. Experimental

The experiments were carried out in an ultrahigh vacuum chamber ( $<10^{-10}$  torr) which has been introduced elsewhere.<sup>18,29</sup> Briefly, a two-stage closed-cycle helium refrigerator coupled with a rotary platform is attached to the main chamber and holds a polished polycrystalline silver mirror serving as a substrate for the ice condensation. With the

combination of the closed-cycle helium refrigerator and a programmable temperature controller, the temperature of the silver mirror can be regulated precisely ( $\pm 0.3$  K) between 10 K and 350 K. A valve and a glass capillary array are used to condense gases on the silver mirror. The actual thickness of the ice samples can be controlled *via* the condensation time and the pressure in the main chamber. In the present studies, the  $\text{H}_2^{18}\text{O}/^{16}\text{O}_2$  ice samples were formed by depositing a  $\text{H}_2^{18}\text{O}/^{16}\text{O}_2$  gas mixture (1 : 1) onto the silver mirror at 12 K. To minimize the contaminations inside the ices, we froze  $\text{H}_2^{18}\text{O}$  (Aldrich, 97%  $^{18}\text{O}$ ) with liquid nitrogen and repeatedly defrosted it in vacuum. The gas reservoir was pumped down to  $2 \times 10^{-7}$  torr before it was filled with about 17 torr  $\text{H}_2^{18}\text{O}$  vapor and 17 torr  $^{16}\text{O}_2$  (99.998%). During the deposition, the pressure in the main chamber was maintained at  $1.7 \times 10^{-8}$  torr for 30 min. We estimated the  $\text{H}_2^{18}\text{O}$  to  $^{16}\text{O}_2$  ratio in the ice to be about 4 : 1. The total sample thickness was about  $120 \pm 20$  nm. The samples were irradiated with 5 keV electrons at 12 K for 180 min at beam currents of 0 nA (blank experiment) and 100 nA by scanning the electron beam over an area of  $1.86 \pm 0.02$  cm<sup>2</sup>. After each irradiation, the sample was kept at 12 K for 60 min and then warmed up at 0.5 K min<sup>-1</sup> to 293 K. The infrared spectra of the samples were measured *on line* and *in situ* by a Fourier Transform infrared spectrometer (Nicolet 510 DX FTIR); the species subliming from the samples were monitored with a quadrupole mass spectrometer (Balzer QMG 420).

## 3. Results

### 3.1 Infrared spectra

We detected the formation of ozone ( $\text{O}_3$ ), hydrogen peroxide ( $\text{H}_2\text{O}_2$ ), hydrotrioxy (HOOO), and dihydrogentrioxide (HOOOH) with infrared spectroscopy. Fig. 1 presents a comparison of the infrared spectra before (dashed line) and after (solid line) the irradiation. The absorptions and assignments of the new peaks are summarized in Table 1. In case of ozone, we were also able to distinguish the isotopomers  $^{16}\text{O}^{18}\text{O}^{16}\text{O}$ ,  $^{16}\text{O}^{16}\text{O}^{18}\text{O}$ , and  $^{16}\text{O}^{16}\text{O}^{16}\text{O}$ . At the end of the irradiation, the  $^{16}\text{O}^{16}\text{O}^{18}\text{O}$  isotopomer is—assuming identical infrared absorption coefficients for all isotopomers—four times as abundant as the  $^{16}\text{O}^{18}\text{O}^{16}\text{O}$  species; likewise, the  $^{16}\text{O}^{16}\text{O}^{16}\text{O}$  is three times as abundant as the total of  $^{16}\text{O}^{16}\text{O}^{18}\text{O}$  and  $^{16}\text{O}^{18}\text{O}^{16}\text{O}$ . Cooper reported a 0.8 MeV proton irradiation study of water–oxygen mixtures.<sup>28</sup> These authors also observed absorptions of  $\text{H}^{16}\text{O}_2$  and  $\text{H}^{18}\text{O}_2$  at 1142 cm<sup>-1</sup> and 1078 cm<sup>-1</sup>, respectively. In our study, these peaks are absent. Instead, we observed a weak absorption at 1107 cm<sup>-1</sup>, which has been reported to be the  $\nu_1$  mode of ozone.<sup>20</sup>

Fig. 2 shows the evolution of the ozone ( $^{16}\text{O}^{16}\text{O}^{16}\text{O}$ ), hydrotrioxy (HOOO), and hydrogen peroxide (HOOH) during the warming up of the sample; both latter bands are too broad to assign the isotopomers individually. Note that the concentrations of  $^{18}\text{O}^{16}\text{O}^{16}\text{O}$  and  $^{16}\text{O}^{18}\text{O}^{16}\text{O}$  are too low to extract temperature dependent profiles. The signal of the HOOO drops immediately with the onset of the warm up; at 100 K, no HOOO radicals could be observed. This is not a result of the sublimation as we cannot detect this radical in the

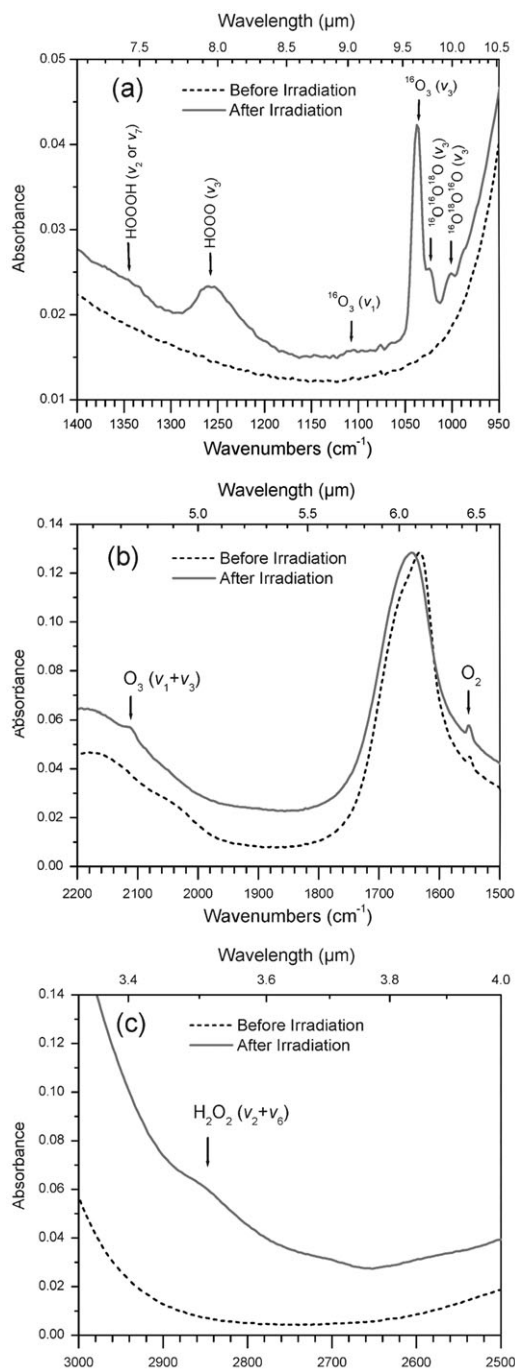


**Fig. 1** Infrared spectra of the  $\text{H}_2^{18}\text{O}/\text{O}_2$  ice mixture before (dashed line) and after the irradiation (solid line) with 5 keV electrons at a current of 100 nA; graphs are shown offset for clarity.

mass spectrometer (see below). The temperature dependent profile of the infrared absorption of the ozone molecule behaves similarly to the one observed in pure oxygen samples.<sup>20</sup> The increase of ozone with the temperature indicates that oxygen atoms trapped in the matrix become mobile and react with molecular oxygen to form additional ozone upon warming. In case of the water–oxygen ices, the ozone intensity increases by about 30% when it is warming up to 40 K before sublimation sets in. At 170 K, most of the ozone sublimed.

**Table 1** Assignment of the new infrared absorption features generated *via* electron irradiation

Absorption/ $\text{cm}^{-1}$	Assignment	Ref.
1003	$^{16}\text{O}^{18}\text{O}^{16}\text{O}$ $\nu_3$ asymmetric stretch	31
1024	$^{16}\text{O}^{16}\text{O}^{18}\text{O}$ $\nu_3$ asymmetric stretch	31
1037 (strong)	$^{16}\text{O}^{16}\text{O}^{16}\text{O}$ $\nu_3$ asymmetric stretch	20, 23, 31
1107 (weak)	$^{16}\text{O}^{16}\text{O}^{16}\text{O}$ $\nu_1$ symmetric stretch	20
1259	HOOO $\nu_3$ OH deformation	28, 32
1350	HOOOH $\nu_2$ and $\nu_7$ HOO bend	33
2113	$\text{O}_3$ $\nu_1 + \nu_3$ combination mode	20, 23
2849	$\text{H}_2\text{O}_2$ $\nu_2 + \nu_6$ combination mode	18

Likewise, the profile of the hydrogen peroxide first increases four-fold up to about 60 K. That is probably because the mobility of OH is increased during the warming.<sup>30</sup> The OH radicals started to combine to form more  $\text{H}_2\text{O}_2$ .

### 3.2 Mass spectra

During the irradiation of the  $\text{H}_2^{18}\text{O}/^{16}\text{O}_2$  ices at 12 K, we observed minor concentrations of molecular hydrogen subliming into the gas phase. It is slightly more than that in the pure water ices irradiated with the same electron currents.<sup>18</sup> During the warming up phase, the  $\text{H}_2^{18}\text{O}/^{16}\text{O}_2$  system depicts strong differences compared to the  $\text{H}_2^{18}\text{O}$  experiments conducted for comparison at identical physical conditions (temperature, electron dose) (Fig. 3). Here, the signal at  $m/z = 2$  ( $\text{H}_2^+$ ) shows three distinct peaks at 15–30 K, 90–145 K and 150–180 K in case of the electron-irradiated pure  $\text{H}_2^{18}\text{O}$ . The signal at 15–30 K originates from minor molecular hydrogen contaminations on the surface layers of the water sample.<sup>18</sup> Ion currents at 150–180 K originate from dissociative ionization of subliming water molecules in the electron impact ionizer, as demonstrated by Zheng *et al.*<sup>18</sup> However, molecular hydrogen was clearly released in the temperature interval from 90 K to 145 K; this finding correlates nicely with the electron irradiation of neat water ices ( $\text{H}_2^{16}\text{O}$ ).<sup>18</sup> Considering the admixture of molecular oxygen, the situation changes dramatically in the irradiated  $\text{H}_2^{18}\text{O}/^{16}\text{O}_2$  ices. During the warm up phase, no significant amount of hydrogen was observed. Quantitatively, the total amount of molecular hydrogen produced during the irradiation and warming up in the  $\text{H}_2^{18}\text{O}/^{16}\text{O}_2$  ices at 12 K is about 10% of that produced in the pure water ices.<sup>18</sup> This finding indicates that the presence of molecular oxygen in water ices drastically reduces the formation of molecular hydrogen. Our result is similar to the MeV proton processing of methane ( $\text{CH}_4$ ) and methane–oxygen (1–2%) ices at 10 K. Here, molecular hydrogen was detected only in pure methane ices, but not in the methane–molecular oxygen matrixes.<sup>34</sup>

We would like to comment now on the formation of the isotopomers of ozone. Fig. 4 shows the mass spectra of water ( $\text{H}_2^{18}\text{O}$ ;  $m/z = 20$ ) (a), molecular oxygen ( $^{16}\text{O}_2$ ;  $m/z = 32$ ) (b) and ozone ( $^{16}\text{O}_3$ ;  $m/z = 48$ ) (c). After irradiation, the  $\text{O}_2$  ( $m/z = 32$ ) signal between 155 and 180 K is much stronger than that in the blank experiment. The dashed lines were taken from the blank experiment and are shown for comparison. The ion current profile of ozone shows three distinct peaks. At 25–40 K and 145–15 K, it is evident that signal at  $m/z = 48$

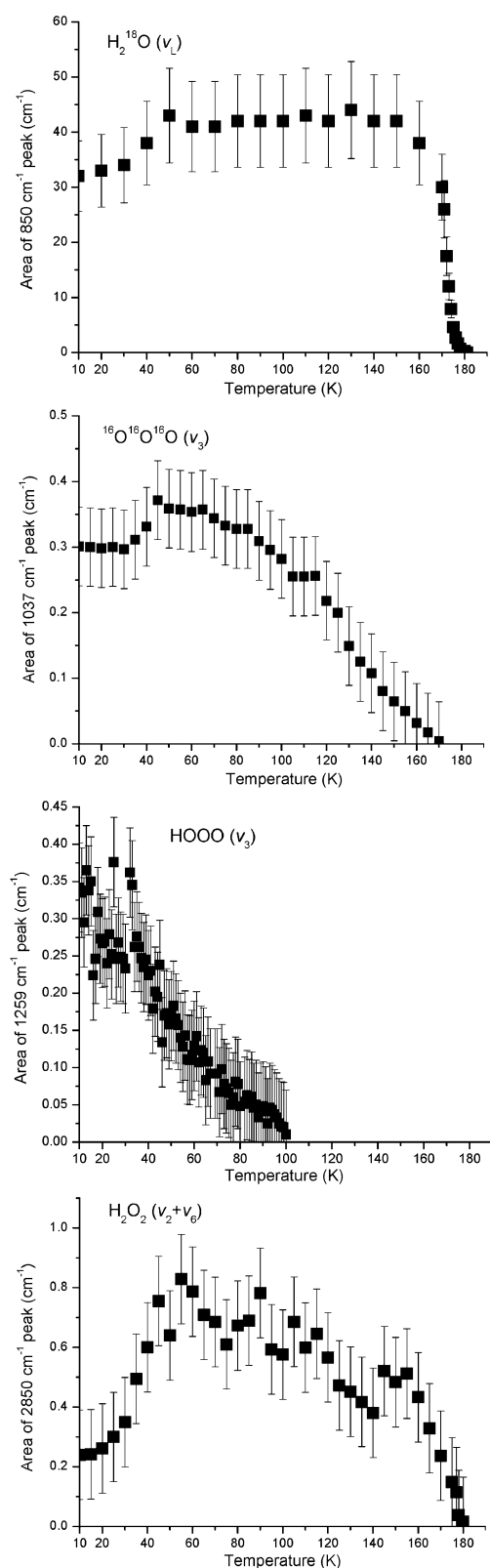


**Fig. 2** Temperature dependent profiles of the absorptions of ozone (<sup>16</sup>O<sup>16</sup>O<sup>16</sup>O isotopomer), hydrogen trioxy (HOOO), and hydrogen peroxide.

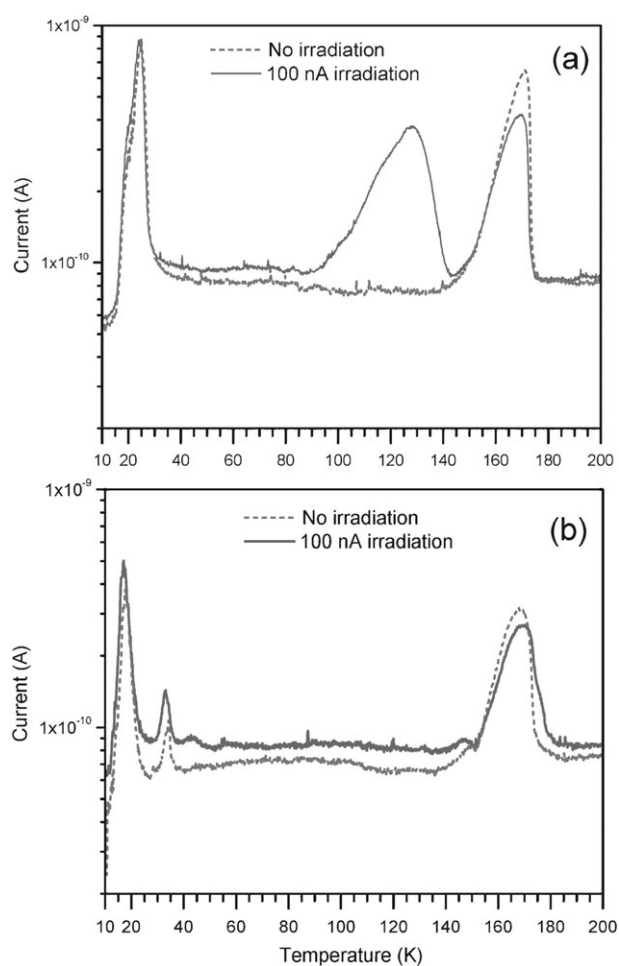


**Fig. 3** Mass spectral data of molecular hydrogen (H<sub>2</sub>) recorded *via* its molecular peak at *m/z* = 2 during the warm up period of the irradiated samples. (a) Pure H<sub>2</sub><sup>18</sup>O ice, (b) H<sub>2</sub><sup>18</sup>O/<sup>16</sup>O<sub>2</sub> ice mixture. The dashed lines indicate the blank experiments, the solid lines the irradiation experiments.

originates from ion-molecule reactions of O<sub>2</sub> with O<sub>2</sub><sup>+</sup> in the electron impact ionizer.<sup>20</sup> However, the signal in the range of 160 K to 180 K is not present in the blank experiment. As a matter of fact, the ion current of <sup>16</sup>O<sub>2</sub><sup>+</sup> at *m/z* = 32 of the irradiated sample also shows a pronounced peak in the same temperature interval. This indicates that the peak at *m/z* = 48 in the temperature interval from 160 K to 180 K actually arises from subliming, newly formed ozone molecules. Note that the corresponding <sup>18</sup>O<sup>16</sup>O<sub>2</sub> isotopomer (*m/z* = 50) has been observed only in the irradiation experiment (Fig. 5). Assuming identical ionization cross sections and fragmentation patterns, we can also integrate the ion currents of the newly formed <sup>16</sup>O<sub>3</sub> and <sup>18</sup>O<sub>2</sub><sup>16</sup>O species. We find that <sup>18</sup>O<sup>16</sup>O<sub>2</sub> is about three times less abundant than <sup>16</sup>O<sub>3</sub>. It should be stressed that we did not detect the formation of <sup>18</sup>O<sub>2</sub><sup>16</sup>O (*m/z* = 52) or <sup>18</sup>O<sub>3</sub> (*m/z* = 54) in our experiment. The peaks emerging in the temperature ranges of 160 K–175 K and 175 K to 183 K could be attributed to <sup>18</sup>O<sup>16</sup>O<sub>2</sub> (Fig. 5).

It is important to comment on the observed hydrogen peroxide isotopomers. Recall that we can expect the formation of H<sup>18</sup>O<sup>18</sup>OH *via* eqn (6) [*m/z* = 38, 37, 36], H<sup>16</sup>O<sup>18</sup>OH *via*

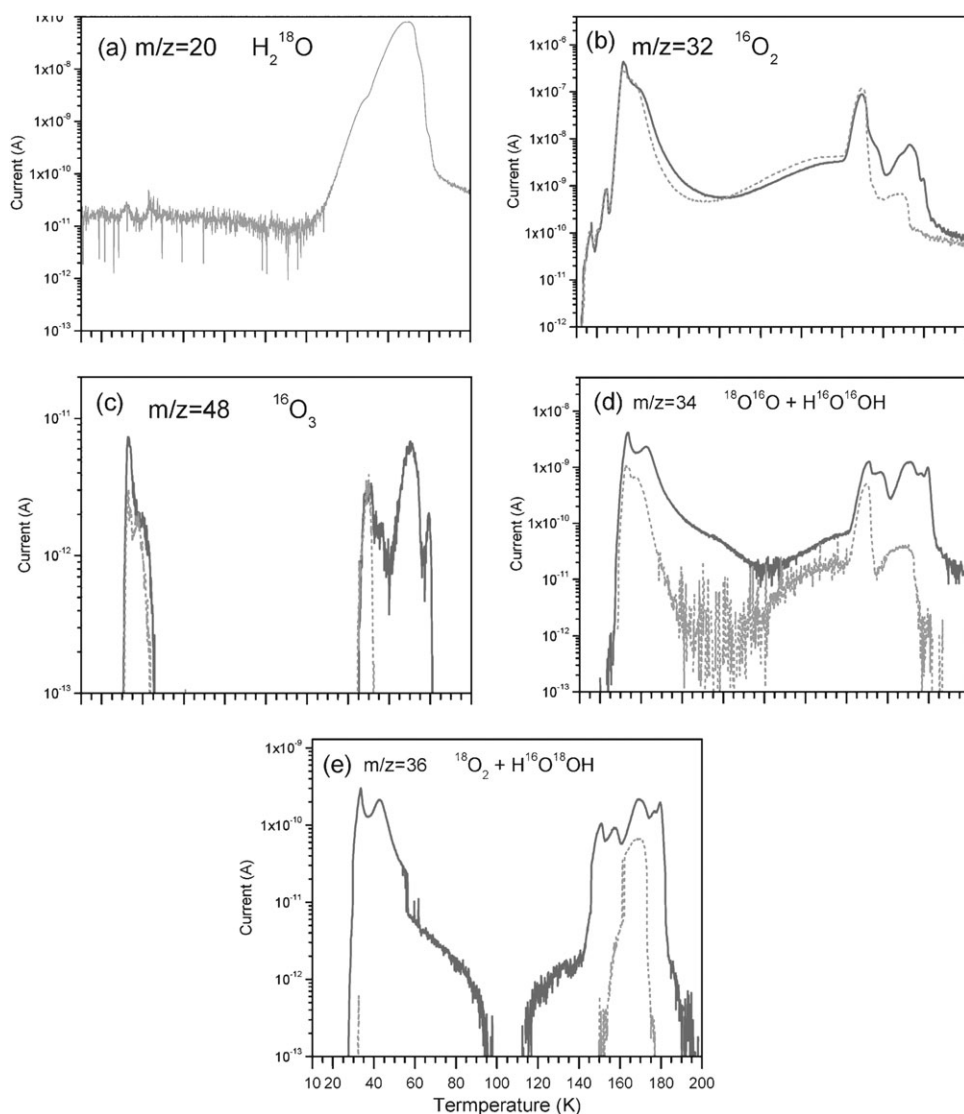


**Fig. 4** Ion currents of species released into the gas phase during the warming up. (a)  $\text{H}_2^{18}\text{O}$  ( $m/z = 20$ ), (b)  $^{16}\text{O}_2$  ( $m/z = 32$ ), (c)  $^{16}\text{O}_3$  ( $m/z = 48$ ), (d)  $^{18}\text{O}^{16}\text{O}$  and  $\text{H}_2^{18}\text{O}^{16}\text{O}$  ( $m/z = 34$ ), and (e)  $^{18}\text{O}_2$  and  $\text{H}_2^{18}\text{O}^{16}\text{O}$  ( $m/z = 36$ ). Dashed lines: blank; solid lines: irradiation experiment.

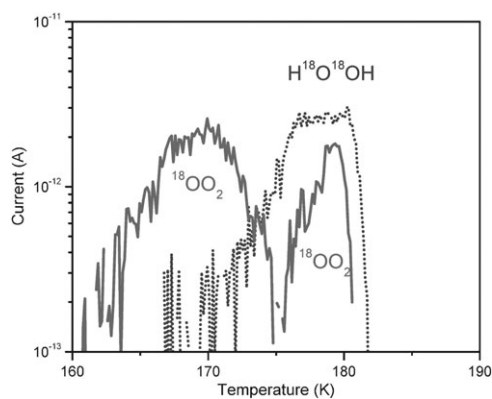


**Fig. 5** Ion currents of newly formed  $^{18}\text{O}^{16}\text{O}^{16}\text{O}$  ( $m/z = 50$ ) and  $\text{H}_2^{18}\text{O}_2$  ( $m/z = 38$ ) released into the gas phase during the warm up phase.

eqn (7) [ $m/z = 36, 35, 34$ ], and  $\text{H}^{16}\text{O}^{16}\text{OH}$  if two hydrogen atoms add stepwise to molecular oxygen [ $m/z = 34, 33, 32$ ]. The fragmentation of the distinct hydrogen peroxide isotopomers clearly complicates the situation. Starting with the highest  $m/z = 38$  ( $\text{H}^{18}\text{O}^{18}\text{OH}$ ), we can clearly identify this species in Fig. 5 at the  $2\text{--}3 \times 10^{-12}$  A level. The signal at  $m/z = 36$  mainly originates from the molecular ion of  $\text{H}^{16}\text{O}^{18}\text{OH}$ , and ionized  $^{18}\text{O}_2$ , since it is much higher than that of  $\text{H}^{18}\text{O}^{18}\text{OH}$ . Finally, we would like to have a detailed look at  $m/z = 34$  (Fig. 4e), which can arise from the ion of the  $\text{H}^{16}\text{O}^{16}\text{OH}$  and from singly ionized  $^{18}\text{O}^{16}\text{O}$ . Recall that  $\text{H}^{16}\text{O}^{16}\text{OH}$  can only be released at temperatures higher than 160 K.<sup>18</sup> In Fig. 4d, we see significant ion counts up to the  $10^{-9}$  A level from  $\text{H}^{16}\text{O}^{16}\text{OH}$ . At lower temperatures—between 60 K and 100 K—we can see a broad feature that can be attributed to subliming  $^{18}\text{O}^{16}\text{O}$ . We did not observe any signal at  $m/z$  higher than 50.

## 4. Discussion

The proposed reaction mechanisms have to account for results R1–R6 as extracted from the mass spectrometer and the infrared data. In addition, the temporal profiles of the hydrogen peroxide, hydrogen trioxy radical, and  $^{16}\text{O}^{16}\text{O}^{16}\text{O}$  together with the corresponding pseudo first-order fits (Fig. 6) have to be accounted for in the proposed reaction mechanisms:

(R1) the total amount of molecular hydrogen produced during the irradiation and warming up in the  $\text{H}_2^{18}\text{O}/^{16}\text{O}_2$  ices at 12 K is about 10% of that produced in the pure water ices.

(R2) the mass spectrometer detected the formation of  $^{18}\text{O}^{16}\text{O}$ ,  $^{16}\text{O}^{16}\text{O}$ , and  $^{18}\text{O}^{18}\text{O}$ .

(R3) the experiments could verify the synthesis of  $\text{H}^{16}\text{O}^{16}\text{OH}$ ,  $\text{H}^{16}\text{O}^{18}\text{OH}$ , and  $\text{H}^{18}\text{O}^{18}\text{OH}$ —the first isotopomer

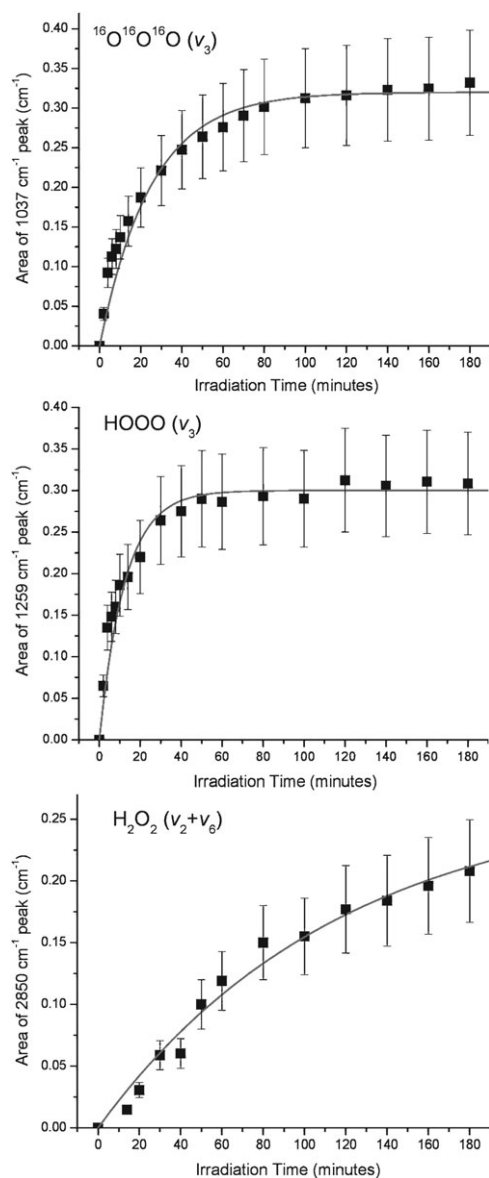


**Fig. 6** Temporal evolutions and pseudo first-order fits of the absorptions of three reaction products in the irradiated  $\text{H}_2^{18}\text{O}/\text{O}_2$  ice mixture:  $^{16}\text{O}^{16}\text{O}^{16}\text{O}$ , HOOO, and  $\text{H}_2\text{O}_2$ .

being formed in about 300–500 times higher abundances than  $\text{H}^{18}\text{O}^{18}\text{OH}$ . The infrared data could not distinguish these isotopomers.

(R4) we detected only the  $^{16}\text{O}_3$  and  $^{16}\text{O}_2^{18}\text{O}$  isotopomers of ozone with a ratio of about 3 : 1 *via* the mass spectrometer in the sublimation phase. The infrared spectra identified three isotopomers of ozone:  $^{16}\text{O}^{16}\text{O}^{16}\text{O}$ ,  $^{16}\text{O}^{16}\text{O}^{18}\text{O}$ , and  $^{16}\text{O}^{18}\text{O}^{16}\text{O}$ . Both latter have identical mass spectra. At the end of the irradiation, the  $^{16}\text{O}^{16}\text{O}^{18}\text{O}$  isotopomer is four times as abundant than the  $^{16}\text{O}^{18}\text{O}^{16}\text{O}$  species;  $^{16}\text{O}^{16}\text{O}^{16}\text{O}$  is three times more abundant than  $^{16}\text{O}^{16}\text{O}^{18}\text{O}$  plus  $^{16}\text{O}^{18}\text{O}^{16}\text{O}$ , corroborating the mass spectrum data.

(R5) based on the temperature dependence of the infrared absorptions of the hydrogen peroxide and of the  $^{16}\text{O}^{16}\text{O}^{16}\text{O}$  isotopomer, we inferred the existence of oxygen atoms and of hydroxyl radicals. In the matrix, the lifetime of  $\text{O}(^1\text{D})$  varies strongly from 32 s to 780 ms.<sup>35</sup> We can therefore conclude that after the isothermal phase all  $\text{O}(^1\text{D})$  atoms are relaxed to their  $^3\text{P}$  ground state.

(R6) based on the infrared spectra, the signal of the HOOO radical was found to decrease with rising temperature

To account for these experimental findings, we propose the following mechanistic model (Fig. 7). Upon interaction of the electron with a  $\text{H}_2^{18}\text{O}$  molecule, the latter undergoes unimolecular decomposition to form a hydrogen atom and a hydroxyl radical ( $^{18}\text{OH}$ ). If two  $\text{H}_2^{18}\text{O}$  molecules are in the correct geometrical orientation, two  $^{18}\text{OH}$  can recombine to form  $\text{H}^{18}\text{O}^{18}\text{OH}$  (R3). A second channel is the fragmentation to  $^{18}\text{O}(^1\text{D})$  plus molecular hydrogen. Also, molecular oxygen ( $^{16}\text{O}_2$ ) interacts with the energetic electron and fragments to two oxygen atoms ( $^{16}\text{O}$ ). The presence of free  $^{16}\text{O}$  and  $^{18}\text{O}$  oxygen atoms is supported by the detection of their recombination product,  $^{18}\text{O}^{16}\text{O}$  (R2). We also observed the formation of  $^{18}\text{O}^{18}\text{O}$  (R2). Since the decomposition of molecular oxygen to liberate a  $^{16}\text{O}$  oxygen atom is more efficient than the loss of an  $^{18}\text{O}$  oxygen atom from a  $\text{H}_2^{18}\text{O}$  molecule, the  $^{16}\text{O}$  oxygen concentration is much larger than those of  $^{18}\text{O}$  oxygen, so that statistically  $^{18}\text{O}$  recombined with an abundant  $^{16}\text{O}$  instead of  $^{18}\text{O}$ .

What is the fate of the liberated oxygen atoms besides the formation of  $^{18}\text{O}^{16}\text{O}$  and—the undetectable—recycling of

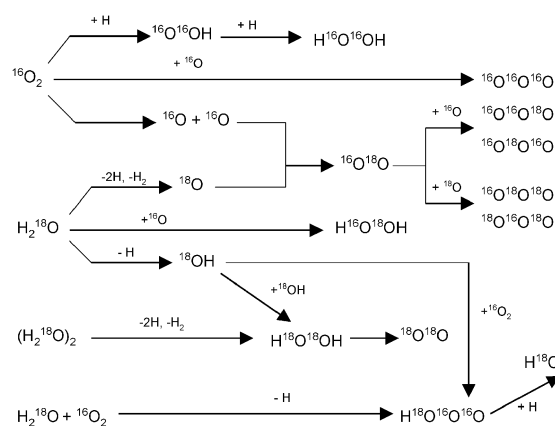


**Fig. 7** Proposed reaction model in electron-irradiated  $\text{H}_2^{18}\text{O}/\text{O}_2$  ice mixtures.

$^{16}\text{O}^{16}\text{O}$ ? Based on the observed isotope patterns and intensities of  $^{16}\text{O}^{16}\text{O}^{16}\text{O}$ ,  $^{16}\text{O}^{16}\text{O}^{18}\text{O}$ , and  $^{16}\text{O}^{18}\text{O}^{16}\text{O}$ , and higher concentration of  $^{16}\text{O}$  compared to  $^{18}\text{O}$ , we can extract likely formation routes of the ozone isotopomers. As demonstrated in pure oxygen ices subjected to an electron irradiation,<sup>20</sup> the temporal evolution of  $^{16}\text{O}^{16}\text{O}^{16}\text{O}$  follows pseudo-first order kinetics *via* eqn (9).

$$[^{16}\text{O}^{16}\text{O}^{16}\text{O}](t) = a \times (1 - e^{-kt}) \quad (9)$$

This is also the case in the present experiments (Fig. 6). We could achieve pseudo first order fits with a rate constant  $k = 4.0 \pm 0.5 \times 10^{-2} \text{ min}^{-1}$  and a pre-exponential factor of  $0.32 \pm 0.02 \text{ cm}^{-1}$ . In addition,  $^{16}\text{O}$  can react with  $^{18}\text{O}^{16}\text{O}$  either by adding to the  $^{18}\text{O}$  or  $^{16}\text{O}$  yielding  $^{16}\text{O}^{18}\text{O}^{16}\text{O}$  and  $^{16}\text{O}^{16}\text{O}^{18}\text{O}$ , respectively, in a multi-step reaction sequence. Since  $^{16}\text{O}^{16}\text{O}$  is more abundant than the  $^{16}\text{O}^{18}\text{O}$  intermediate, we would expect that  $^{16}\text{O}^{16}\text{O}^{16}\text{O}$  is formed preferentially to  $^{16}\text{O}^{16}\text{O}^{18}\text{O}$  and  $^{16}\text{O}^{18}\text{O}^{16}\text{O}$ . This has been confirmed experimentally (R4). In theory,  $^{18}\text{O}$  atoms can also react with  $^{18}\text{O}^{16}\text{O}$  either by adding to the  $^{18}\text{O}$  or  $^{16}\text{O}$  yielding  $^{18}\text{O}^{18}\text{O}^{16}\text{O}$  and  $^{18}\text{O}^{16}\text{O}^{18}\text{O}$ , respectively. However, these isotopomers were not observed—strongly supporting the conclusion that under our experimental conditions, the liberation of  $^{16}\text{O}$  from molecular oxygen is much more efficient than the release of  $^{18}\text{O}$  from water. Recent dynamics calculations suggest that ground state oxygen atoms can only abstract a hydrogen atom from a water molecule.<sup>21</sup> A computational study suggested that only  $\text{O}(^1\text{D})$  could yield hydrogen peroxide *via* an oxywater intermediate.<sup>36</sup> The detection of  $\text{H}^{16}\text{O}^{18}\text{OH}$  (R3) in our experiments agrees with the theoretical calculations. On the other hand, we detected  $\text{H}^{16}\text{O}^{16}\text{OH}$  in our experiments. How can this molecule be formed? We may propose a reaction of hydrogen atoms with  $^{16}\text{O}^{16}\text{O}$  to form a  $\text{H}^{16}\text{O}^{16}\text{O}$  intermediate; a second hydrogen atom can react *via* a fast, barrier-less atom–radical reaction to form  $\text{H}^{16}\text{O}^{16}\text{OH}$ . We would like to stress that we did not observe the  $\text{H}^{16}\text{O}^{16}\text{O}$  intermediate in our experiment. This could be due to the large concentration of mobile hydrogen atoms formed *via* reaction (1). In our experiments, the total amount of molecular hydrogen produced during the irradiation and warming up in the  $\text{H}_2^{18}\text{O}/^{16}\text{O}_2$  ices at 12 K is about 10% of that produced in the pure water ices (R1). Therefore, the hydrogen atoms must be ‘trapped’ by a molecule—most likely  $^{16}\text{O}^{16}\text{O}$ —reacting then in two fast steps to  $\text{H}^{16}\text{O}^{16}\text{OH}$  (R1/R3). If these processes are very fast, a pseudo first-order rate constant might be rationalized as observed experimentally (Fig. 6). Considering the 300–500 fold higher yield of  $\text{H}^{16}\text{O}^{16}\text{OH}$  compared to  $\text{H}^{18}\text{O}^{18}\text{OH}$ —which may be formed formally *via* pseudo first order decomposition of a water dimer—we might suggest that, at least in water–oxygen ices, the formation of hydrogen peroxide proceeds predominantly *via* hydrogen addition pathways to molecular oxygen.

Finally, we would like to address briefly the formation of  $\text{HOOH}$  and  $\text{HOO}$ . In polar, water-rich matrices, it is difficult to extract the detailed isotopic patterns of these molecules since the absorption of  $\text{HOOO}$  is very broad and of  $\text{HOOH}$  very weak (Fig. 1). Considering Fig. 6, a pseudo first order graph could fit the temporal profile of  $\text{HOOO}$  ( $k = 8.5 \pm 1.0 \times 10^{-2} \text{ min}^{-1}$  and a pre-exponential factor of  $a = 0.30$

$\pm 0.02 \text{ cm}^{-1}$ ). This reaction could be induced by a neighboring water–molecular oxygen complex. Inducing an oxygen–hydrogen bond rupture, the hydroxyl radical could react with the molecular oxygen to form the hydrotrioxy radical. Upon warming up the sample, the absorptions decrease rapidly. This could either indicate a reaction of mobile hydrogen atoms to form the dihydrotrioxy molecule or a decomposition of the hydrotrioxy radical, possibly to a hydroxyl radical and molecular oxygen atom.<sup>37</sup>

## 5. Conclusions

In summary, we conducted a detailed infrared spectroscopy and mass spectrometry study on the electron irradiation of  $\text{H}_2^{18}\text{O}/\text{O}_2$  ice mixtures. We detected the formation of molecular hydrogen, isotopically substituted oxygen molecules  $^{18}\text{O}^{18}\text{O}$  and  $^{16}\text{O}^{18}\text{O}$ , ozone ( $^{16}\text{O}^{16}\text{O}^{16}\text{O}$ ,  $^{16}\text{O}^{16}\text{O}^{18}\text{O}$ , and  $^{16}\text{O}^{18}\text{O}^{16}\text{O}$ ), hydrogen peroxide ( $\text{H}^{18}\text{O}^{18}\text{OH}$ ,  $\text{H}^{16}\text{O}^{16}\text{OH}$  and  $\text{H}^{16}\text{O}^{18}\text{OH}$ ), hydrotrioxy ( $\text{HOOO}$ ), and dihydrotrioxy ( $\text{HOOOH}$ ) and also proposed reaction pathways to form these molecules in low temperature ices. Most important, we found that the irradiation production of molecular hydrogen was reduced significantly compared to pure water ice due to the existence of  $\text{O}_2$  trapping the mobile hydrogen atoms effectively as hydrogen peroxide. Our studies also confirmed that a water molecule under irradiation is mainly dissociated to a hydrogen atom and a hydroxyl radical.

## Acknowledgements

This work was financed by the NASA Astrobiology Institute under Cooperative Agreement NNA04CC08A at the University of Hawaii-Manoa (WZ) and by the US National Science Foundation (NSF; AST-0507763; DJ, RIK). We are grateful to Ed Kawamura (University of Hawaii at Manoa, Department of Chemistry) for his electrical work.

## References

- 1 M. H. Moore and R. L. Hudson, *Icarus*, 2000, **145**, 282–288.
- 2 R. E. Johnson and T. I. Quickenden, *J. Geophys. Res., [Planets]*, 1997, **102**, 10985–10996.
- 3 G. Leto, M. E. Palumbo and G. Strazzulla, *Nucl. Instrum. Methods Phys. Res., Sect. B*, 1996, **116**, 49.
- 4 P. A. Gerakines, W. A. Schutte and P. Ehrenfreund, *Astron. Astrophys.*, 1996, **312**, 289–305.
- 5 G. A. Kimmel and T. M. Orlando, *Phys. Rev. Lett.*, 1995, **75**, 2606.
- 6 M. Shi, R. A. Baragiola, D. E. Grosjean, R. E. Johnson, S. Jurac and J. Schou, *J. Geophys. Res., [Atmos.]*, 1995, **100**, 26387–26396.
- 7 A. Bar-Nun, G. Herman, M. L. Rappaport and Y. Mekler, *Surf. Sci.*, 1985, **150**, 143.
- 8 W. L. Brown, W. M. Augustyniak, E. Simmons, K. J. Marcantonio, L. J. Lanzerotti, R. E. Johnson, J. W. Boring, C. T. Reimann, G. Foti and V. Pirronello, *Nucl. Instrum. Methods Phys. Res.*, 1982, **198**, 1–8.
- 9 W. L. Brown, W. M. Augustyniak, E. Brody, B. Cooper, L. J. Lanzerotti, A. Ramirez, R. Evatt and R. E. Johnson, *Nucl. Instrum. Methods*, 1980, **170**, 321–325.
- 10 W. L. Brown, W. M. Augustyniak and L. J. Lanzerotti, *Phys. Rev. Lett.*, 1980, **45**, 1632–1635.
- 11 J. F. Cooper, R. E. Johnson, B. H. Mauk, H. B. Garrett and N. Gehrels, *Icarus*, 2001, **149**, 133–159.
- 12 J. F. Cooper, E. R. Christian, J. D. Richardson and C. Wang, *Earth Moon Planets*, 2003, **92**, 261–277.
- 13 D. C. Jewitt and J. Luu, *Nature*, 2004, **432**, 731.

- 14 R. A. Sultanov and N. Balakrishnan, *Astrophys. J.*, 2005, **629**, 305–310.
- 15 C. J. Bennett, C. S. Jamieson, Y. Osamura and R. I. Kaiser, *Astrophys. J.*, 2005, **624**, 1097–1115.
- 16 P. D. Holtom, C. J. Bennett, Y. Osamura, N. J. Mason and R. I. Kaiser, *Astrophys. J.*, 2005, **626**, 940–952.
- 17 G. Leto and G. A. Baratta, *Astron. Astrophys.*, 2003, **397**, 7–13.
- 18 W. Zheng, D. Jewitt and R. I. Kaiser, *Astrophys. J.*, 2006, **639**, 534–548.
- 19 W. Zheng, D. Jewitt and R. I. Kaiser, *Astrophys. J.*, 2006, **648**, 753–761.
- 20 C. J. Bennett and R. I. Kaiser, *Astrophys. J.*, 2005, **635**, 1362–1369.
- 21 M. Braunstein, R. Panfili, R. Shroll and L. Bernstein, *J. Chem. Phys.*, 2005, **122**.
- 22 M. J. Redmon, G. C. Schatz and B. C. Garrett, *J. Chem. Phys.*, 1986, **84**, 764.
- 23 B. D. Teolis, M. J. Loeffler, U. Raut, M. Fam and R. A. Baragiola, *Astrophys. J.*, 2006, **644**, L141–L144.
- 24 J. R. Spencer, W. M. Calvin and M. J. Person, *J. Geophys. Res., [Atmos.]*, 1995, **100**, 19049.
- 25 J. R. Spencer and W. M. Calvin, *Astron. J.*, 2002, **124**, 3400–3403.
- 26 J. M. Greenberg, C. E. P. M. van de Bult and L. J. Allamandola, *J. Phys. Chem.*, 1983, **87**, 4243–4260.
- 27 T. Owen, ASSL vol. 83: Strategies for the Search for Life in the Universe, 1980.
- 28 P. D. Cooper, M. H. Moore and R. L. Hudson, *J. Phys. Chem. A*, 2006, **110**, 7985–7988.
- 29 C. J. Bennett, C. Jamieson, A. M. Mebel and R. I. Kaiser, *Phys. Chem. Chem. Phys.*, 2004, **6**, 735–746.
- 30 C. Laffon, S. Lacombe, F. Bournel and P. Parent, *J. Chem. Phys.*, 2006, **125**, 204714.
- 31 W. E. Thompson and M. E. Jacox, *J. Chem. Phys.*, 1989, **91**, 3826.
- 32 B. Nelander, A. Engdahl and T. Svensson, *Chem. Phys. Lett.*, 2000, **332**, 403.
- 33 A. Engdahl and B. Nelander, *Science*, 2002, **295**, 482–483.
- 34 R. I. Kaiser, G. Eich, A. Gabrysch and K. Roessler, *Astrophys. J.*, 1997, **484**, 487–498.
- 35 H. H. Mohammed, *J. Chem. Phys.*, 1990, **93**, 412–415.
- 36 Y. Ge, K. Olsen, R. I. Kaiser and J. D. Head, *ASTROCHEMISTRY: From Laboratory Studies to Astronomical Observations*, Honolulu, Hawaii (USA), 2006.
- 37 K. Suma, Y. Sumiyoshi and Y. Endo, *Science*, 2005, **308**, 1885–1886.



Save valuable time searching for that elusive piece of vital chemical information.

Let us do it for you at the Library and Information Centre of the RSC.

We are your chemical information support, providing:

- Chemical enquiry helpdesk
- Remote access chemical information resources
- Speedy response
- Expert chemical information specialist staff

Tap into the foremost source of chemical knowledge in Europe and send your enquiries to

[library@rsc.org](mailto:library@rsc.org)